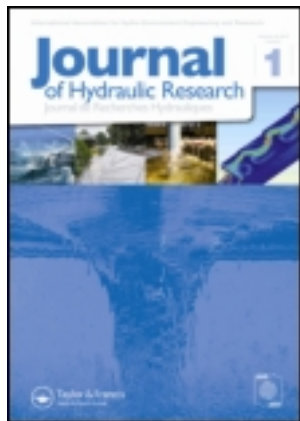


This article was downloaded by: [University of Ljubljana]

On: 29 February 2012, At: 04:34

Publisher: Taylor & Francis

Informa Ltd Registered in England and Wales Registered Number: 1072954 Registered office: Mortimer House, 37-41 Mortimer Street, London W1T 3JH, UK



Journal of Hydraulic Research

Publication details, including instructions for authors and subscription information:
<http://www.tandfonline.com/loi/tjhr20>

Study of velocity field at model sideweir using visualization method

Gorazd Novak ^a, Franc Steinman ^b, Matej Müller ^c & Tom Bajcar ^d

^a Chair of Fluid Mechanics with Laboratory, Faculty of Civil and Geodetic Engineering, University of Ljubljana, Hajdrihova 28, Ljubljana, Slovenia

^b Chair of Fluid Mechanics with Laboratory, Faculty of Civil and Geodetic Engineering, University of Ljubljana, Hajdrihova 28, Ljubljana, Slovenia E-mail:

^c Chair of Fluid Mechanics with Laboratory, Faculty of Civil and Geodetic Engineering, University of Ljubljana, Hajdrihova 28, Ljubljana, Slovenia E-mail:

^d Faculty of Mechanical Engineering, University of Ljubljana, Aškerčeva 6, Ljubljana, Slovenia E-mail:

Available online: 19 Jan 2012

To cite this article: Gorazd Novak, Franc Steinman, Matej Müller & Tom Bajcar (2012): Study of velocity field at model sideweir using visualization method, Journal of Hydraulic Research, 50:1, 129-133

To link to this article: <http://dx.doi.org/10.1080/00221686.2011.648766>

PLEASE SCROLL DOWN FOR ARTICLE

Full terms and conditions of use: <http://www.tandfonline.com/page/terms-and-conditions>

This article may be used for research, teaching, and private study purposes. Any substantial or systematic reproduction, redistribution, reselling, loan, sub-licensing, systematic supply, or distribution in any form to anyone is expressly forbidden.

The publisher does not give any warranty express or implied or make any representation that the contents will be complete or accurate or up to date. The accuracy of any instructions, formulae, and drug doses should be independently verified with primary sources. The publisher shall not be liable for any loss, actions, claims, proceedings, demand, or costs or damages whatsoever or howsoever caused arising directly or indirectly in connection with or arising out of the use of this material.



Technical note

Study of velocity field at model sideweir using visualization method

GORAZD NOVAK, PhD Student, *Chair of Fluid Mechanics with Laboratory, Faculty of Civil and Geodetic Engineering, University of Ljubljana, Hajdrihova 28, Ljubljana, Slovenia.*

Email: gorazd.novak@fgg.uni-lj.si (author for correspondence)

FRANC STEINMAN, Professor, *Chair of Fluid Mechanics with Laboratory, Faculty of Civil and Geodetic Engineering, University of Ljubljana, Hajdrihova 28, Ljubljana, Slovenia.*

Email: franci.steinman@fgg.uni-lj.si

MATEJ MÜLLER, PhD Student, *Chair of Fluid Mechanics with Laboratory, Faculty of Civil and Geodetic Engineering, University of Ljubljana, Hajdrihova 28, Ljubljana, Slovenia.*

Email: matej.mueller@fgg.uni-lj.si

TOM BAJCAR, Assistant Professor, *Faculty of Mechanical Engineering, University of Ljubljana, Aškerčeva 6, Ljubljana, Slovenia.*

Email: tom.bajcar@fs.uni-lj.si

ABSTRACT

A visualization method was employed for accurate non-intrusive measurement of velocity fields at a physical model of a sharp-crested rectangular sideweir under subcritical flow. The experimental observation of velocity vectors at various horizontal planes over the entire width of the main channel confirms that the flow conditions at sideweir are non-uniform. The coefficients of non-uniform velocity distribution were in the range from 1 to 1.1. The present study focuses on the relation between the longitudinal components of the overflow velocities and the corresponding cross-sectional average velocities in the main channel, detailed as a function of flow depth and of location along the sideweir crest. For different sideweir geometries, these coefficients varied between 1 and 1.2.

Keywords: Laboratory experiment, model study, open channel flow, sideweir, velocity field, visualization

1 Introduction

Sideweirs are hydraulic structures for diverting discharge from a main channel to a lateral. They are widely used to control discharge in irrigation, sewer, and flood management systems.

The performance of sideweirs was investigated from the pioneering work of De Marchi (1934), seminal work of Hager (1982, 1983, 2010), to recent work of Emiroglu *et al.* (2011). Most concentrated on the total lateral outflow Q_s , the free surface profile, and the discharge coefficient C_d . In contrast, this work focuses on the experimental determination of the velocity field of a model sideweir using a non-intrusive visualization method. The velocity-related terms are included in the fundamental one-dimensional equation for spatially-varied flow. Its energy-approach-based form includes the kinetic energy coefficient

α , while the momentum-approach-based equation includes the overflow velocity component parallel to main channel axis U , the average channel flow velocity V , and the momentum coefficient β . The measured velocity fields indicate either $U = V$, as assumed in the constant energy approach, or $U > V$, as implied by the momentum approach. Using non-intrusive visualization causes accurate flow observations result, whereas intrusive instrumentation causes significant flow perturbations.

Recent works based on the constant energy approach are by Singh *et al.* (1994), Swamee *et al.* (1994), Borghei *et al.* (1999), or Rosier *et al.* (2010). The effect of specific energy variation was considered by Yüksel (2004) and Venutelli (2008). Representative works based on the momentum approach are by El-Khashab and Smith (1976), Hager and Volkart (1986), Lee and Holley (2002), or May *et al.* (2003).

Revision received 7 December 2011/Open for discussion until 31 August 2012.

2 Methodology

The velocity field of sideweir flow can be determined using either pathlines or streaklines (Kline 1969). The non-intrusive computer-aided visualization method of Bajcar *et al.* (2009) was employed. This method determines the vector velocity field from a scalar field of pollutant concentrations using the sequence of grayscale images of the observed flow. This approach is based directly on the physical advection–diffusion equation representing the basic connection between pollutant concentration and the flow kinematics as

$$\frac{\partial N}{\partial t} + \frac{\partial(Nv_i)}{\partial x_i} = D\nabla^2 N \quad (1)$$

By knowing concentration N , its derivatives, and the molecular diffusivity D of the pollutant, the only unknown is velocity, i.e. its components v_i in the directions x_i . The pollutant is introduced to the fluid, then illuminated and digitally recorded on a high-speed film. The grayscale values of these images correspond to the relation $A \propto N$, where A is an average grayscale value in the selected window of pixels on a grayscale image. Both temporal and spatial derivatives of concentration in Eq. (1) are approximated by knowing the duration between two successive images and the dimensions of grayscale images. The approximated spatial derivatives are then numerically determined.

The method differs from other visualization methods based on the correlation of successive flow images. Furthermore, the method does not require timelines, as employed by Dargahi (1997), and works well with pollutants such as dye, bubbles, or particles. Herein, the electrolysis-generated hydrogen bubbles were employed as the most suitable pollutant for a small testing facility.

Okamoto *et al.* (1971) specified the uncertainties of the hydrogen bubble visualization as (1) horizontal streamline shift by

buoyancy, (2) entry length for bubble acceleration, (3) wake flow behind wire, (4) centripetal force in curved flow, and (5) decaying time by absorption. The optimum bubble diameter, which is comparable to the wire diameter, is 0.06–0.15 mm (Okamoto *et al.* 1971, Tropea *et al.* 2007). Following the latter, a wire of 0.5 mm diameter was used. Also, 1 kg of common salt was added per 3 m³ of water to produce bubbles of less than 100 μ m (Dargahi 1997). To address the above issues, a preliminary test was conducted to experimentally optimize the wire position, to adjust the image acquisition equipment, and to calibrate the settings for numerical calculation. Calibration tests with plastic and cork particles were performed as well. The resulting velocities from the calibrated visualization method V_c agreed well with these observed with floats V_f , i.e. $V_c/V_f = 1(\pm 3\%)$.

3 Experimental setup

Six types of Plexiglas sideweirs involving various crest lengths L and crest heights p were tested in a glass-walled horizontal flume 7.5 m long, 0.2 m wide, and 0.5 m deep (Fig. 1). The flow was always subcritical. The inflow Q_1 and outflow Q_2 discharges were measured with V-notch weirs, while $Q_s = Q_1 - Q_2$. Free surface elevations were measured using a point gauge of ± 0.1 mm reading accuracy and photos of laser-induced vertical sections of the flow. The flow depth h_2 at the downstream sideweir end was adjusted for each Q_1 to provide modular discharge Q_s and sufficient overflow depth $h - p \geq 19$ mm (Emiroglu *et al.* 2011) to avoid surface tension effects. The main hydraulic conditions are given in Table 1. The study was based on a relatively narrow channel, yet the dimensionless parameters were mostly within the ranges of previous investigations (Table 2).

The velocity fields were recorded at five horizontal planes, located by z_w above the sideweir bed. Four distances z_w were

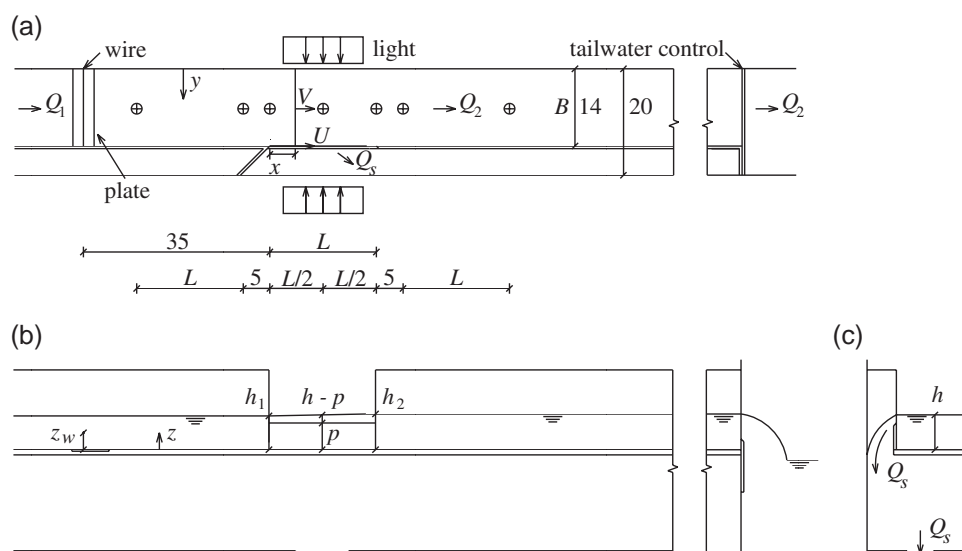


Figure 1 Definition sketch of experimental set-up (in cm): (a) plan, (b) elevation, and (c) section $x/L = 0.5$; points mark the locations of water level measurement

Table 1 Main test parameters, with $h-p$ measured at $L/2$

Weir Type	$L = 25, p = 12$ [cm]			$L = 20, p = 12$ [cm]			$L = 20, p = 10$ [cm]			$L = 15, p = 10$ [cm]			$L = 15, p = 7.5$ [cm]			$L = 10, p = 7.5$ [cm]		
	a	b	c	a	b	c	a	b	c	a	b	c	a	b	c	a	b	c
Q_1 (l/s)	6.34	6.94	7.83	5.45	6.62	7.59	5.29	6.01	6.62	4.54	5.45	6.06	3.82	4.52	5.30	3.31	3.97	4.71
Q_{s_s} (l/s)	1.09	1.36	1.79	0.83	1.35	1.83	1.05	1.29	1.52	0.89	1.09	1.29	1.09	1.24	1.34	0.84	0.84	0.92
Q_1/Q_s (-)	0.17	0.20	0.23	0.15	0.20	0.24	0.20	0.22	0.23	0.20	0.20	0.21	0.28	0.27	0.25	0.25	0.21	0.20
F_1 (-)	0.28	0.31	0.33	0.25	0.28	0.31	0.29	0.31	0.34	0.25	0.28	0.30	0.29	0.33	0.36	0.26	0.29	0.32
h_1 (cm)	13.73	13.91	14.25	13.69	14.28	14.63	11.98	12.44	12.59	12.06	12.58	12.84	9.66	10.01	10.41	9.52	9.99	10.36
h_2 (cm)	13.96	14.21	14.63	13.88	14.42	14.92	12.20	12.60	12.89	12.21	12.78	13.10	9.84	10.24	10.71	9.59	10.07	10.46
$h-p$ (cm)	1.89	2.05	2.47	1.90	2.37	2.79	2.06	2.48	2.73	2.19	2.67	2.90	2.24	2.60	3.05	2.05	2.49	2.93

Table 2 Ranges of measured parameters from previous and present studies

Authors	B (cm)	L (cm)	p (cm)	S_o (%)	Q_1 (l/s)	B/L (-)	F_1 (-)	Q_s/Q_1 (-)
El-Khashab and Smith (1976)	46	120,230	10–25	Varied	≤ 220	0.2–0.38	≤ 1.2	0.3–0.8
Balmforth and Sarginson (1983)	100	46–76	4–12	–	–	0.46–0.76	Varied	–
Hager and Volkart (1986)	30	100	0–20	-4 to 5	0–45	0.3	0.3–2	–
Singh <i>et al.</i> (1994)	25	10–20	6–12	–	10–14	1.25–2.5	0.2–0.4	–
Swamee <i>et al.</i> (1994)	50	20–50	0–60	0	20–100	1–2.5	0.1–0.93	–
Borghesi <i>et al.</i> (1999)	30	20–70	1,10,19	-0.5 to 1	35–100	0.43–1.5	0.1–0.9	–
Pinheiro and Silva (1999)	50	150,200	20	–	25–150	0.25–0.33	< 1	0.25–0.75
May <i>et al.</i> (2003)	21–60	20–100	5–25	0	–	0.21–3	< 1	0.08–1
Present study	14	10–25	7.5–12	0	4–7.8	0.56–1.4	0.28–0.34	0.20–0.27

selected in relation to p , i.e. $z_w/p = 0, 1/3, 2/3$, and 1, respectively, while the fifth plane was located 5 mm below the free surface. The illumination was placed at z_w on both channel sides to illuminate a 5 mm high horizontal layer, reaching over the entire sideweir width. The distance between the wire and the upstream sideweir end was constant. To maintain recording quality, the voltage of the adjustable DC source was increased for higher z_w . The camera was placed vertically above the channel. For each test, some 1500 images were recorded at 300 frames/s and then converted into grayscale images. Sets of 500 images were employed to determine the velocity vectors in each pixel along a selected section. Three sets were averaged to obtain the plane velocity components V_x, V_y , and U_x, U_y . The standard deviation of the velocity components was on average 0.6. Various parameters of the numerical calculation can be adjusted; the pixel size proved to be an important factor, and was adjusted for each z_w .

4 Results

4.1 Velocity fields

For all sideweir geometries and combinations of the inflow Q_1 and flow depth h_2 , the measured velocity fields were non-uniform. Figure 2 shows a typical velocity field for $z_w = p$. As expected, the measured longitudinal velocity components decrease with distance from water surface and also in the direction x , while the outflow angle increases with x . At the downstream sideweir end, weak standing waves were formed

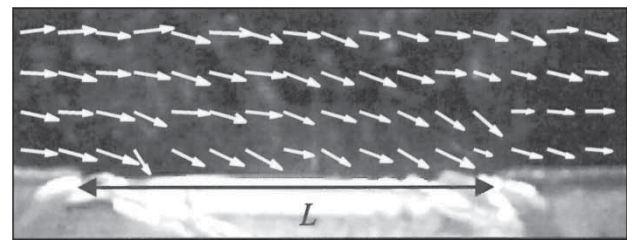


Figure 2 Typical plane velocity field

above the crest. At the end of the sideweir, velocities near the main channel bed decreased.

4.2 Velocity distribution coefficients

In general, the coefficients α and β increased along the sideweir from 1.02 to 1.08 and from 1.01 to 1.03, respectively, in agreement with $\alpha = [1 + (q/(Q/B))^2]^{4/3}$ of Hager (1982), with q being the unit overflow discharge. Also, values α at given x/L increased from type (a) to type (c) test runs. At cross sections $0.25L$ upstream and downstream of the sideweir, respectively, the coefficients α were similar to those at $x/L = 0$ and 1, respectively.

The coefficients β were close to unity in all tests. The data confirm that “approximately, β can be replaced by unity” (Hager 1983). However, β was significantly below the constant 1.23, as proposed by May *et al.* (2003), who suggested $\beta = 0.725 + 0.275(U/V)$.

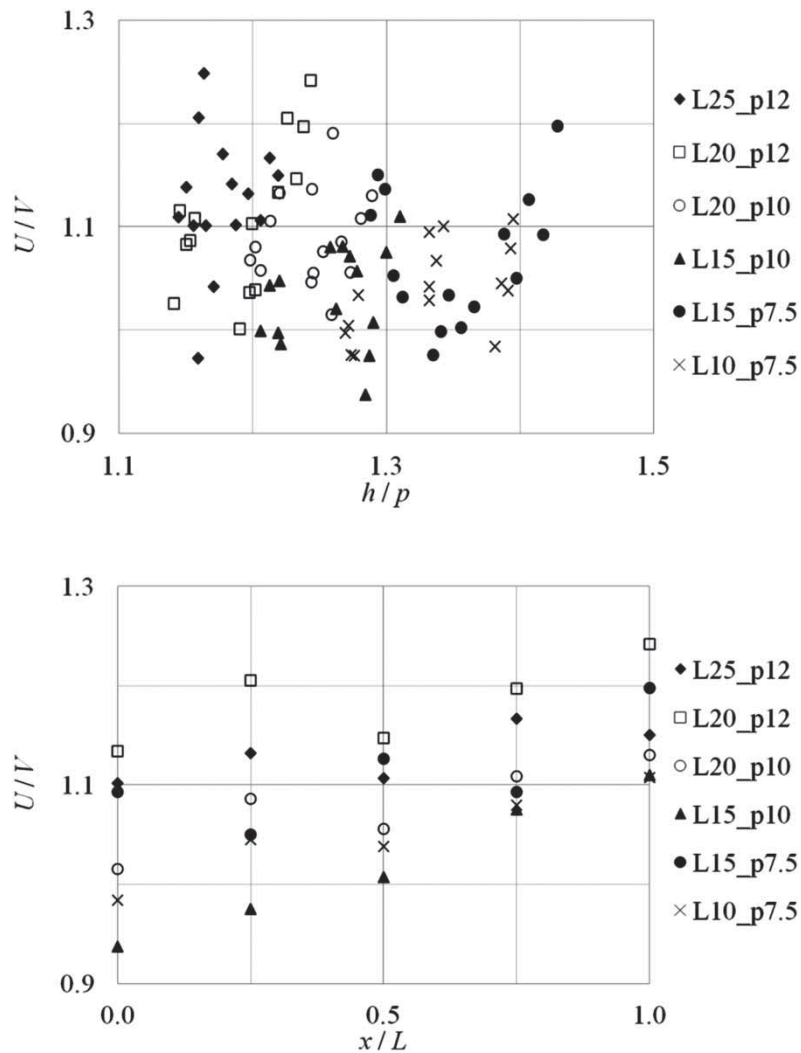


Figure 3 Values of U/V versus (a) h/p and (b) x/L for maximum inflow discharges

4.3 Relation U/V

Values of $U/V = f(h/p)$ were measured for h/p values ranging from 1.15 to 1.4, resulting in $U/V \cong 1-1.2$ (Fig. 3a). For a given geometry, the U/V ratio increases with h/p . Figure 3(b) also shows that U/V increases with the distance from the upstream end of the sideweir. It is evident that $U/V > 1.1$ at $x/L = 1$ for all sideweir geometries tested.

5 Conclusions

A visualization method was employed for accurate non-intrusive measurement of the velocity fields at sharp-crested model sideweirs in subcritical flow. The data indicate that the velocity distribution is highly non-uniform. Both the kinetic energy and momentum correction coefficients vary along the sideweir on the average from 1.02 to 1.08, and 1.01 to 1.03, respectively, in agreement with an available proposal. Furthermore, the ratio of the longitudinal overflow velocity component and the average sideweir velocity varies essentially with the ratio of flow depth to weir height. This ratio also varies along the sideweir. The present

data confirm the assumption of non-uniform velocity distribution, as implied by the momentum approach. The results of this study apply for calibrating numerical models of sideweir flow.

Notation

- F_1 = approach flow Froude number (–)
- L = length of sideweir (m)
- p = height of sideweir crest (m)
- Q_1 = approach flow discharge (m^3/s)
- Q_s = discharge over sideweir (m^3/s)
- U = streamwise sideweir velocity component (m/s)
- V = average main channel flow velocity (m/s)
- z_w = observed horizontal plane (m)
- α = kinetic energy correction coefficient (–)
- β = momentum correction coefficient (–)

References

- Bajcar, T., Širok, B., Eberlinc, M. (2009). Quantification of flow kinematics using computer-aided visualization. *J. Mech. Eng.* 55(4), 215–223.

- Balmforth, D.J., Sarginson, E.J. (1983). The effects of curvature in supercritical side weir flow. *J. Hydraulic Res.* 21(5), 333–343.
- Borghei, S.M., Jalili, M.R., Ghodsian, M. (1999). Discharge coefficient for sharp-crested side weir in subcritical flow. *J. Hydr. Eng.* 125(10), 1051–1056.
- Dargahi, B. (1997). Generation of coherent structures in turbulent boundary layer. *J. Eng. Mech.* 123(7), 686–695.
- De Marchi, G. (1934). Saggio di teoria del funzionamento degli stramazzi laterali (Theory of sideweirs). *L'Energia Elettrica* 11(11), 849–860 [in Italian].
- El-Khashab, A., Smith, K.V.H. (1976). Experimental investigation of flow over side weirs. *J. Hydraulics Div.* ASCE 102(9), 1255–1268.
- Emiroglu, M.E., Agaccioglu, H., Kaya, N. (2011). Discharging capacity of rectangular side weirs in straight open channels. *Flow Measurement and Instrumentation* 22(4), 319–330.
- Hager, W.H. (1982). Die Hydraulik von Verteilkanälen (Hydraulics of distribution channels). *Mitteilungen* 55–56. Versuchsanstalt für Wasserbau, Hydrologie und Glaziologie, ETH Zurich, Zürich [in German].
- Hager, W.H. (1983). Open channel hydraulics of flows with increasing discharge. *J. Hydraulic Res.* 21(3), 177–193.
- Hager, W.H. (2010). *Wastewater hydraulics: Theory and practice*, ed. 2. Springer, Berlin.
- Hager, W.H., Volkart, P.U. (1986). Distribution channels. *J. Hydraulic Eng.* 112(10), 935–952.
- Kline, S.J. (1969). *Film notes for flow visualization*: Nat. Committee for Fluid Mech. Films, Stanford University <http://web.mit.edu/hml/ncfmf/05FV.pdf>.
- Lee, K.-L., Holley, E.R. (2002). *Physical modeling for side-channel weirs*. CRWR Online Report 02-2. Center for Research in WaterResources, The University of Texas at Austin. <http://www.crwr.utexas.edu/reports/pdf/2002/rpt02-02.pdf> (8.3.2011).
- May, R.W.P., Bromwich, B.C., Gasowski, Y., Rickard, C.E. (2003). *Hydraulic design of side weirs*. Thomas Telford, London.
- Okamoto, Y., Hanawa, J., Kameoka, T. (1971). Visualization techniques of closed conduit flows by hydrogen bubble methods. *Bulletin Japan Society of Mech. Engineers* 14(76), 1088–1094.
- Pinheiro, A., Silva, I.N. (1999). *Discharge coefficient of side weirs. Experimental study and comparative analysis of different formulas* [online]. <http://www.iahr.org/membersonly/grazproceedings99/pdf/B072.pdf> (25.8.2011).
- Rosier, B., Boillat, J.L., Schleiss, A. (2010). Semi-empirical model for channel bed evolution due to lateral discharge withdrawal. *J. Hydraulic Res.* 48(2), 161–168.
- Singh, R., Manivannan, D., Satyanarayana, T. (1994). Discharge coefficient of rectangular side weirs. *J. Irrig. Drain. Eng.* 120(4), 814–819.
- Swamee, P.K., Pathak, S.K., Mohan, M., Agrawal, S.K., Ali, M.S. (1994). Subcritical flow over rectangular side weir. *J. Irrig. Drain. Eng.* 120(1), 212–217.
- Tropea, C., Yarin, A.L., Foss, J.F., eds. (2007). *Springer handbook of experimental fluid mechanics*. Springer, Berlin.
- Venutelli, M. (2008). Method of solution of non-uniform flow with the presence of rectangular side weir. *J. Irrig. Drain. Eng.* 134(6), 840–846.
- Yüksel, E. (2004). Effect of specific energy variation on lateral overflows. *Flow Measurement and Instrumentation* 15(5–6), 259–269.